ARCHIVES OF ACOUSTICS
9, 1-2, 121-130 (1984)

ECHOGRAPHIC SIGNAL PROCESSING

A. HERMENT, P. PERONNEAU

Hopital Broussais, (96, rue Didot, 75674 Paris, France)

G. DEMOMENT

L.S.S. C.N.R.S. E.S.E. (Plateau du Mouton, Gif-sur-Yvette, France)

The information received from the insonified tissues is strongly filtered by the echograph. The acoustic probe technology and the simplified processing of the echoes are mainly responsible for this loss of information.

Two deconvolution methods have been designed to correct partly the echograph characteristics. The first one, which is a sub-optimal Kalman filter, is easy to implement and offers short calculation time. It is consequently well dedicated to quasi real time imaging. The second one is slower but extracts from the processed signal some geometric information on the medium interfaces. This information may be used to obtain a more precise estimation of the coefficients of reflexion in the medium and thus to characterize the tissues by their acoustic impedance.

The ability of the methods to process real echographic signals is demonstrated on the rabbit eye and the human humeral artery.

1. Introduction

The performance of echographs has significantly been improved during the last years. The storage of the image and the numerical processing of the echoes have simplified the medicist's work. However, the treatment of the $R-F$ signals in the echograph is still very crude and a large amount of the received information is lost. Deconvolution technics, however, are able to restore partly this information by correction of the appliance's characteristics. These technics lead to the obtention of better defined images [2, 6]. In addition, if the medium geometry may be taken into account during signal processing, they allow the characterization of the tissues by their acoustic impedance [1, 5].

Two deconvolution processes are presented, both of which use the principle of "process-identification" and have been designed to combine a good improvement in the echograph discrimination with a convenient noise immunity in order to fit echographic signal characteristics.

2. "On line" deconvolution by sub-optimal Kalman filtering

The principle of the algorithm is explained in Fig. 1. The successive samples of the received signal S_n are introduced into the algorithm. After a delay of treatment, the different values E_n of the deconvoluted signal are obtained one by one at the input frequency.

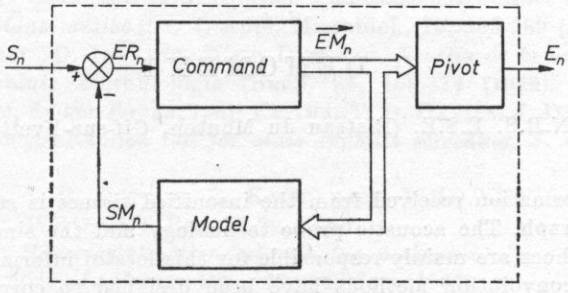

Fig. 1. "On-line" deconvolution : principle

2.1. Error estimation

At instant n the signal $\boldsymbol{EM}_n$ is a rough estimation of the deconvoluted signal. The algorithm will try to forecast from its knowledge, that is to say the echograph impulse response $\boldsymbol{h}$ and $\boldsymbol{EM}_n$, the value of the most probable incoming sample S_n. For this purpose the convolution at the instant n between the echograph impulse response and the estimated deconvoluted signal is computed.

$$\boldsymbol{SM}_n = \boldsymbol{h}^t \cdot \boldsymbol{EM}_n. \tag{1}$$

The received sample S_n is then compared with this value and an error ER_n is obtained.

$$ER_n = S_n - SM_n. \tag{2}$$

2.2. Initialisation of next $\boldsymbol{EM}_n$

From this error, a new estimation of the deconvoluted signal is calculated as follows:

$$\boldsymbol{EM}_{n+1} = \Phi \cdot \boldsymbol{EM}_n - \lambda \cdot ER_n. \tag{3}$$

2.2.1. State transition matrix

The Φ operator which corresponds to the state transition matrix of the Kalman theory is used to initialise the first coordinate of the new vector $\boldsymbol{EM}_n$, because this value has not been affected by the previous operations. Φ has been chosen to simple shift $\boldsymbol{EM}_n$ and to duplicate its first coordinate:

$$(\boldsymbol{EM}_n)^t = (a, b, c, \ldots, n, 0); \quad (\Phi \boldsymbol{EM}_n)^t = (a, a, b, c, \ldots, n);$$

this means that without new information, the algorithm will suppose that the most probable value of the sample S_{n+1} will be equal to S_n. In other words, it is implicitly considered that the received signal cannot change extremely rapidly. This is effectively the case of the echographic signals which are collected through the acoustic probe acting as a low-pass filter.

2.2.2. Correction vector

The vector λ is chosen as the limit value of the Kalman gain vector [3]. This choice has been made in order to shorten the calculation time and to simplify the implementation of the method. The constant vector λ is independant of the received signal and can be calculated separately from the echograph impulse response and an estimation of the noise variance.

2.3. Extraction of the values E_n of the deconvoluted signal

The different values E_n of the deconvoluted signal are obtained by the extraction of one coordinate of $\boldsymbol{EM}_n$. This operation is done after a certain number of iterations of the loop in the algorithm so that the estimated $\boldsymbol{EM}_n$ has become precise enough.

$$E_n = \boldsymbol{P} \cdot \boldsymbol{EM}_n, \quad \text{with } P^t = (P0, P1, \ldots, P_p, \ldots, P_m), \quad \text{where } \begin{cases} P_p = 1 \\ P_i = 0 \forall i \neq p \end{cases} \tag{5}$$

a large value p will improve the sharpness of the processed signal but will lead to a more important delay between the input and the output of the system.

The algorithm is very fast because it needs no matrix inversion and because the vector λ may be calculated beforehand. The process is sub-optimal since this gain vector is taken as constant: consequently edge-effects are neglected in the deconvolution.

3. "Batch" deconvolution

The second method [4] is schematised in Fig. 2. It is based on overall comparison of the received signal, S, with a synthetized waveform, SM, generated by the computer. The construction of SM in the algorithm takes into account the known characteristics of the echograph: the acoustic device impulse response, h, and some unknown properties of the examined structures: position,

angulation and curvature of the interfaces, together with the value of their coefficient of reflexion.

The test of comparison has been designed to work with noisy input signals, and uses the properties of the correlation function.

Finally, the deconvoluted signal is reconstructed from the results of the test and from the different parameters used to built SM.

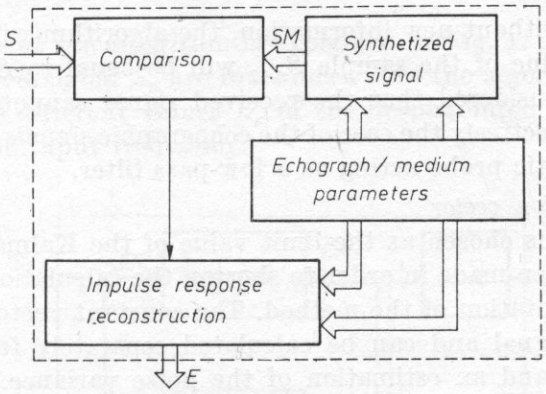

Fig. 2. "Batch" deconvolution : principle

3.1. Synthesis of SM

Two points have to be considered in the synthesis of the signal SM:

1. An increased number of parameters lead to a more sophisticated modelisation of the tissue but lengthens computation time.

2. These parameters have to be defined such as two different sets of them generate two different signals SM, in order to get a single solution to the identification of the insonified medium. Taking into account these two points, it has been chosen to construct SM under the following form

$$SM(p \cdot \Delta T) = \sum_{p=1}^{P} r_p^i \cdot h^{j,k}(p\Delta T - \theta_p^l), \tag{6}$$

where p corresponds to the order of the digital sample, P represents the number of samples in the signal and ΔT the sampling period.

$h^{j,k}$ characterizes the echo shape and depends in quite a complex way on the orientation and on the curvature of the interfaces. The analytical expression of $h^{j,k}$ from the parameter j and k is extremely difficult to establish. This is the reason why we used, in the implementation of the algorithm, a matrix of signals $h^{j,k}$ recorded on calibrated targets of known angulation and curvature which has been stored in the computer memory.

3.2. Test of comparison

The correlation function $C_{S,SM}$ between S and SM is computed and its symmetry with respect to a vertical axis is tested. Effectively, it can be demon-

strated from the properties of the correlation function that if $C_{S,SM}$ posseses a vertical symmetry, then SM is related to S by a multiplying constant. To test the symmetry, the ratio R is used:

$$R = \frac{[\int C_{S,SM}(\eta) \cdot C_{S,SM}(\tau - \eta)\, d\eta]_{\tau=0}}{[\int C_{S,SM}(\tau) \cdot C_{S,SM}(\tau - \mu)\, d\tau]_{\mu=0}}.$$

R which represents the ratio of the value of the autoconvolution function of $C_{S,SM}$ at the origin to the energy of this function will approach the value of one when the symmetry increases.

3.3. Reconstruction of the deconvoluted signal

When the maximum value of R has been determined, the corresponding parameters used to buit SM indicate the angulation and the curvature of each interface localised. This information allows correction of the apparent value of the coefficient of reflexion distorted by the medium geometry.

4. Experimentation on the eye

The method is now applied to the treatment of a series of signals collected on a rabbit eye. The eye was placed in a water tank, immediately after removing and insonified by a 5 MHz probe. The signals, collected within an angle of 90°, have been converted into eight-bit words at a frequency of 50 MHz.

4.1. High definition imagery of the eye

Both algorithms have been used to deconvolute the recorded data. The results have been presented in a crude four level greyscale on a variable persistance display. Fig. 3 presents for comparison an image obtained with a conventional echographic treatment of the signals for a 1 MHz bandwith detection and

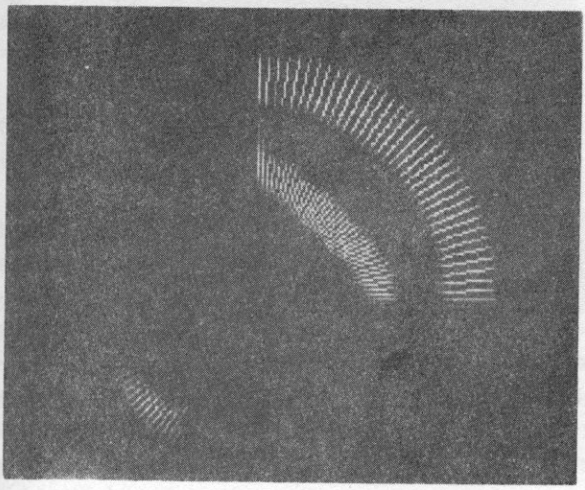

Fig. 3. Echographic image of the rabbit eye

without depth compensation. The image processed by the first algorithm is shown in Fig. 4 and the one obtained by the second method in Fig. 5. The four dotted lines correspond to the front and rear faces of the cornea (not visible in Fig. 3) and of the crystalline lens.

The higher definition of the deconvoluted image allows one 1) to distinguish interfaces masked in the echographic picture such as the two faces of the cornea, and 2) to obtain a better estimation of the shape of the interfaces.

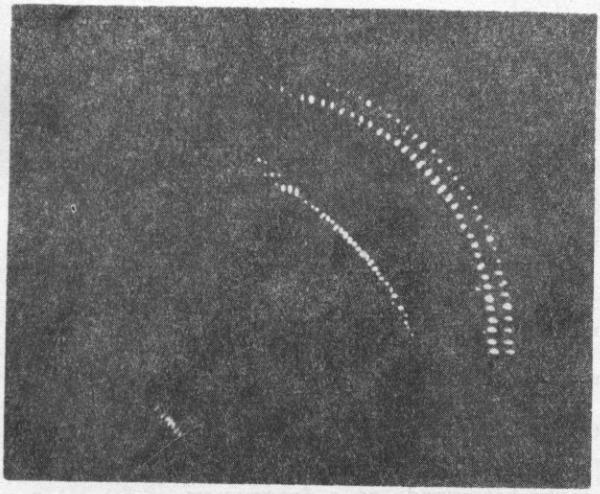

Fig. 4. "On line" deconvolution of the image

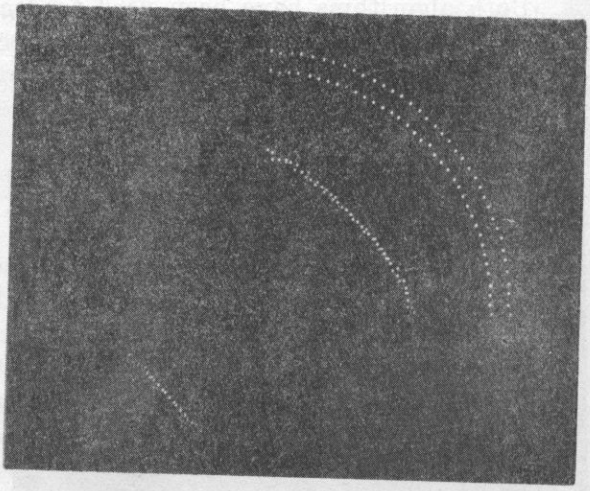

Fig. 5. "Batch" deconvolution of the image

4.2. Acoustic impedance of the eye

The signal recorded when the acoustic beam was centered on the eye axis has been used to calculate the impedance profile of the eye after deconvolution by the second method. It is shown in Fig. 6.

From left to right, one can observe a first zone of unitary normalized impedance which corresponds to the water in which the eye is submerged, then the cornea characterized by a relative impedance of 1.29. The zone with a low normalized impedance of 1.04 corresponds to the aqueous humour. The maximum

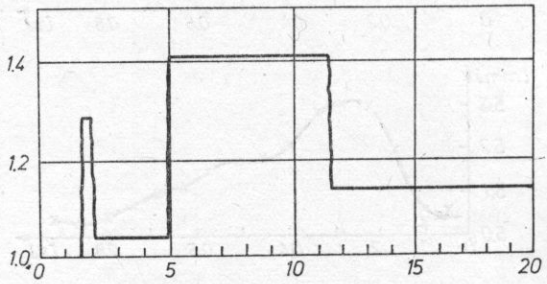

Fig. 6. Impedance profile of the rabbit eye

impedance zone, $Z/Zo = 1.41$ indicates the crossing of the crystalline lens and the last level corresponds to the vitreous humour whose relative impedance was estimated equal to 1.14.

Comparison with the density and propagation speed data given in the literature or measured in our laboratory indicates a good fitting between these calculations and the actual impedance profile.

5. Experimentation on the humeral artery

5.1. Signal recording

The probe was laid on the arm and oriented towards the vessel. Sixteen signals separated by 55 ms were recorded during a cardiac cycle. As for the eye, a 5 MHz probe was used and the signals sampled on eight bits at a rate of 50 MHz.

5.2. Signal processing

The signals were then deconvoluted and the position of the two sides of the second vessel wall was used to follow the wall displacement together with its thickness variations.

The vessel wall thickness is plotted in Fig. 7*a* and the wall position with respect to the probe in Fig. 7*b*. The variations in Fig. 7*b*, which are related in a ratio of 1/2 to the vessel diameter, look very similar to a classical intra-arterial pressure curve, in addition the amplitudes of the observed variations are in full agreement with the ones indicated in the literature. The wall thickness variations in Fig. 7*a* are very well correlated with the one of the previous curve: during systole the enlargment of the diameter corresponds to a thinner vessel wall. The amplitudes of these variations are again very close to the ones announced by the vessel mechanics.

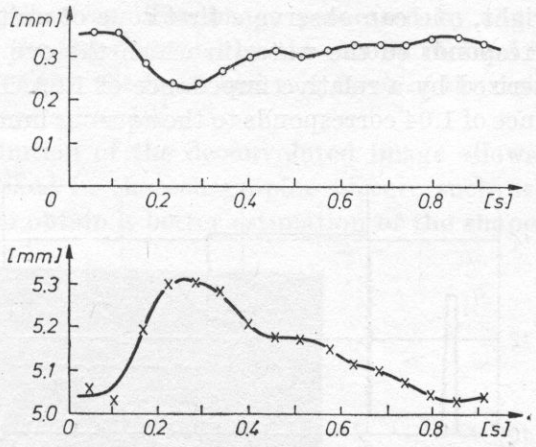

Fig. 7. Study of the humeral artery during one cardiac cycle: *a*) wall thickness variations, *b*) second arterial wall position

6. Conclusion

Two methods for the treatment of echographic signals have been proposed. The first process, derived from Kalman filtering, works "on line" and supplies rapid results with few calculations, it appears consistently well dedicated to the image processing. The second one which is able to take into account some characteristics of the interfaces leads to a finer characterisation of the medium and may be used for tissue characterisation. It is, however, longer and will only be applied when a limited number of structures is to be studied. In vitro experiments on the eye illustrate the performance of the methods and in vivo applications on the vessel show the ability of the methods to process signals recorded in vivo.

References

[1] I. Beretski, *Detection and characterization of atherosclerosis in a human arteria wall by raylographic technique, and in vitro study,* in: Ultrasound in Medicine, D. N. White, R. E. Brown (eds.), Plenum Press Publ., New York, 1977, **3B**, 1597-1612 (1977).

[2] B. Burgogne, J. Pavkovich, *Digital filtering of acoustic images,* in: Acoustical Imaging, J. P. Powers (ed.), Plenum Publ. Co., New York, **11**, 181-207 (1982).

[3] G. Demoment, R. Reynaud, A. Segalen, *Estimation sous-optimale rapide pour la déconvolution en temps réel,* Neuvième Colloque sur le traitement du signal et ses applications "GRETSI", 16-20 mai 1983, Nice.

[4] A. Herment, P. Peronneau, J. P. Moutet, *Echographic signal processing: a method*

taking into account the medium geometry, I.E.E.E. Catalog, I.E.E.E. Computer Society, **82 CH** 1804-4, 331-336, 1982.

[5] J. P. JONES, *Ultrasonic impediography and its applications to tissue characterization,* in: *Recent advances in ultrasound in biomedicine,* D. N. WHITE (ed.), Research Studies Press, Forest Grove, **1**, 131-156 (1977).

[6] A. PAPOULIS, C. CHAMZAS, *Improvement of range resolution by spectral extrapolation,* Ultrasonic Imaging, **1**, 121-135 (1979).